

## Supporting Information

### **Synthetic Light-Curable Polymeric Materials Provide a Supportive Niche for Dental Pulp Stem Cells**

*Kyle H. Vining, Jacob C. Scherba, Alaina M. Bever, Morgan R. Alexander, Adam D. Celiz\*, and David J. Mooney\**

#### **Supplementary Experimental Methods –**

Time-of-flight secondary-ion mass spectrometry (ToF-SIMS) analysis –

ToF-SIMS measurements were conducted using a ToF-SIMS 4 (IONTOF GmbH) instrument operated using a 25 kV Bi<sup>3+</sup> primary ion source exhibiting a pulsed target current of ~1 pA. Samples were scanned at a pixel density of 100 pixels per mm, with 8 shots per pixel over a given area. An ion dose of  $2.45 \times 10^{11}$  ions per cm<sup>2</sup> was applied to each sample area ensuring static conditions were maintained throughout. Both positive and negative secondary ion spectra were collected (mass resolution of >7000), over an acquisition period of 15 scans (the data from which were added together). Owing to the non-conductive nature of the samples, charge compensation was applied in the form of a low energy (20 eV) electron floodgun.

Multivariate analysis - Principal component analysis (PCA) –

The ToF-SIMS spectral data were analyzed using principal component analysis (PCA) as previously described.<sup>[1]</sup> All positive and negative ion peak intensities in a ToF-SIMS spectrum were normalized to the total secondary ion counts to remove the influence of primary ion beam fluctuation. The positive and negative ion intensity data were arranged into one concatenated data matrix. PCA analysis was carried out using the Eigenvector PLS Toolbox 5.2. All datasets were mean-centered and square root mean scaled.

Atomic Force Microscopy (AFM) –

AFM of polymer samples was performed using a Dimension Icon FastScan instrument (Bruker) in PeakForce tapping quantitative nanomechanical mapping (QNM) mode using silicon nitride cantilevers. Force-indentation curves were fit using the DMT model with a pyramid indenter.

Preparation of primary human DPSCs and PDLFs –

DPSCs were acquired commercially from Lonza (Poietics human DPSCs, PT-5025) after 12 passages. According to the manufacturer, over 90% of cells tested positive for CD105, CD166, CD29, CD90, and CD73, and over 95% were negative for CD34, CD45, and CD133. The DPSCs were expanded in culture for 2 passages and then cryopreserved in complete growth media and 7.5% DMSO. DPSCs were thawed for subsequent experiments in aMEM (Gibco) complete media, containing 1% penicillin-streptomycin (P/S), 100  $\mu$ M L-ascorbic acid, and 20% fetal bovine serum. Human periodontal ligament fibroblasts (PDLFs) were commercially obtained from extracted human teeth (Lonza, CC-7049) at passage 2 and cultured in stromal growth media (Lonza) for 2 additional passages prior to cryopreservation as previously described. Incubation conditions were 37C at 5% CO<sub>2</sub>.

Quantitative polymerase chain reaction (qPCR) measurements –

RNA was isolated with PureLink RNA Micro Kit (Invitrogen), quantified by NanoDrop spectrophotometer, and cDNA was reverse-transcribed by iScript Advanced Reverse Transcription Supermix for RT-qPCR (Bio-Rad). Real-time quantitative PCR was performed using CFX96 or CFX394 (Bio-Rad) in duplicate with 10 ng of cDNA and 2x AdvancedSSO SYBR Green Supermix (Bio-Rad) in each reaction. Screening was performed to assess a wide range of genes associated with integrin signaling by using a Bio-Rad PrimePCR Integrin Outside-In Signaling H384 plate. Individual qPCR measurements were repeated on at least three replicate samples using Bio-Rad PrimePCR primers. Relative gene expression was

computed by the delta-delta Ct method, which compared Ct values to a control sample and reference gene (GAPDH). See Table S3 for list of individual gene primers.

#### Micro-computed tomography imaging (MicroCT)

MicroCT images were acquired at the Harvard Center for Nanoscale Systems with a tungsten filament in reflection mode (105 kV, 205 uA, 4 frames per projection). Following 3D reconstruction on VG studio, the coronal pulp in each tooth was segmented to calculate the mineralized volume of reparative dentin.

#### Supplementary Reference

- [1] A. D. Celiz, J. G. W. Smith, A. K. Patel, R. Langer, D. G. Anderson, D. A. Barrett, L. E. Young, M. C. Davies, C. Denning, M. R. Alexander, *Biomaterials Science* **2014**, *2*, 1604.

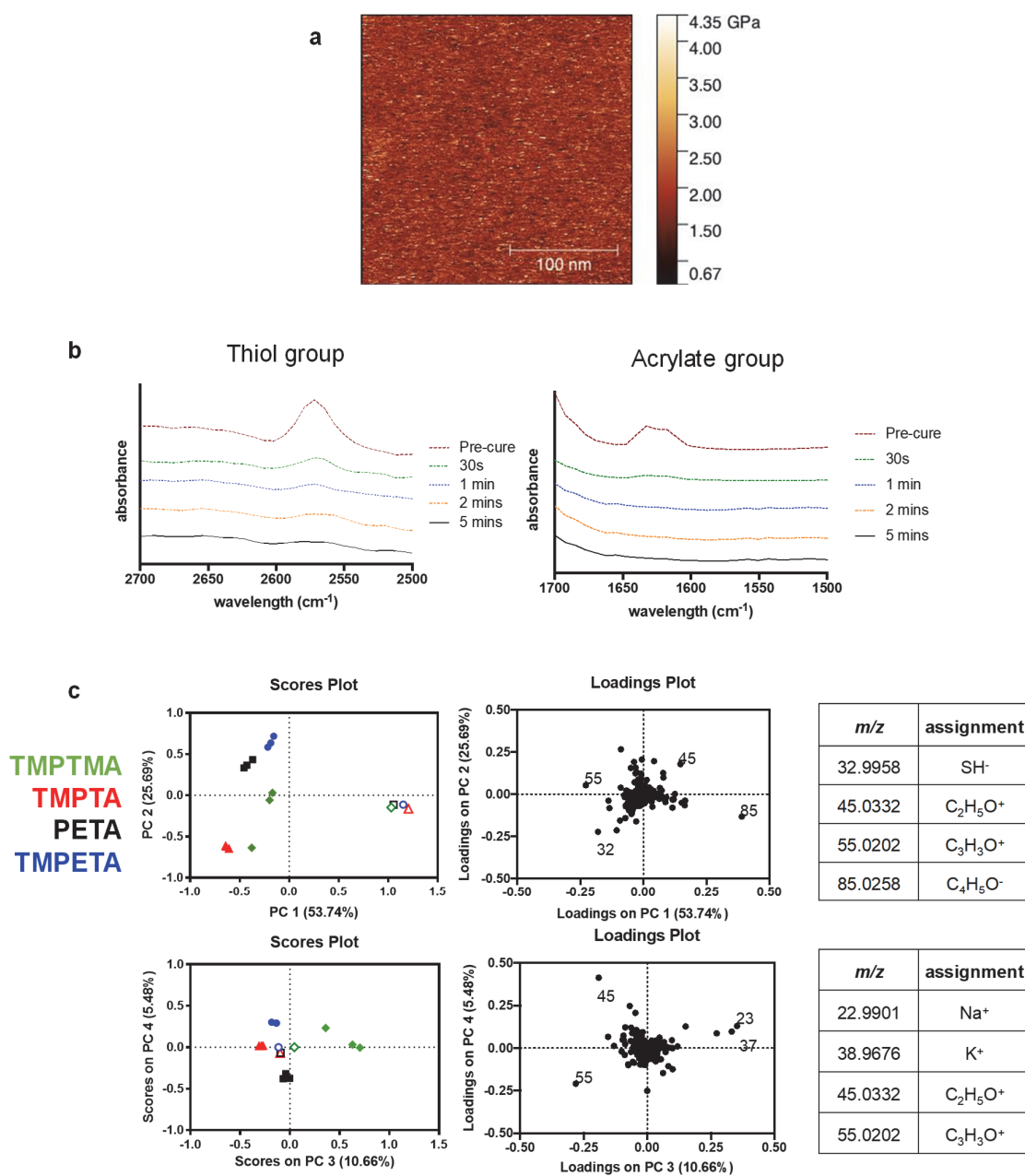


**Figure S1.** Physicochemical characterizations of thiol-ene-crosslinked triacrylate polymers.

A) Representative spectrum of atomic force microscopy mechanical measurements of TMPTA, which showed high elastic moduli ( $\sim 2$  GPa) similar to TCP and dentin  $\sim 10$  GPa, scale bar 100 nm. B) The residual acrylate and thiol chemical groups were measured on the surface of thiol-ene polymerized-TMPTA by Fourier-transform infrared spectroscopy, which showed significant attenuation of the acrylate and thiol peaks after curing. C) Comparison of the surface chemistry of arrayed (open symbols) and scaled-up polymers TMPTMA (green

diamond), TMPTA (red triangle), PETA (black square), and TMPETA (blue circle) was performed using principal component analysis (PCA) of the respective ToF-SIMS spectra. PCA revealed significant differences in surface chemistry between samples with principal component 1 represented the majority of chemical variance (53%) which was assigned to the substrate background poly(2-hydroxyethyl methacrylate) (pHEMA) moieties in the arrayed samples and thiol functionality present in the scaled-up polymers.

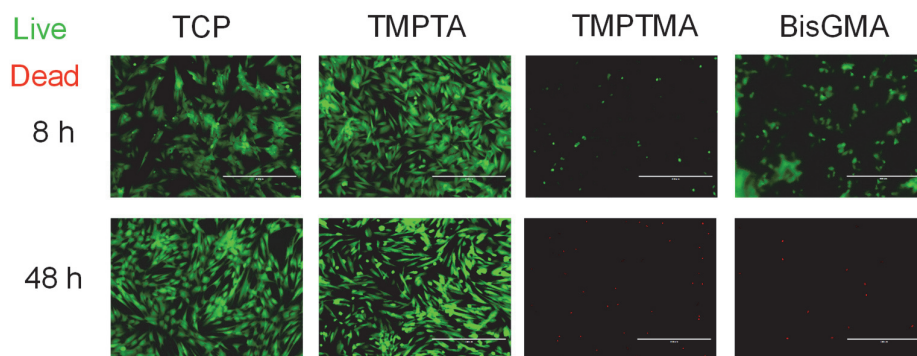


**Figure S2.** Live-dead staining at 8 and 48 hours showed that cells adhered to TMPTA exhibited similar viability as TCP, but significantly fewer viable cells were present on TMPTMA and BisGMA. Live – calcein (green), Dead – ethidium homodimer-1 (red). Scale bar 400  $\mu\text{m}$ .

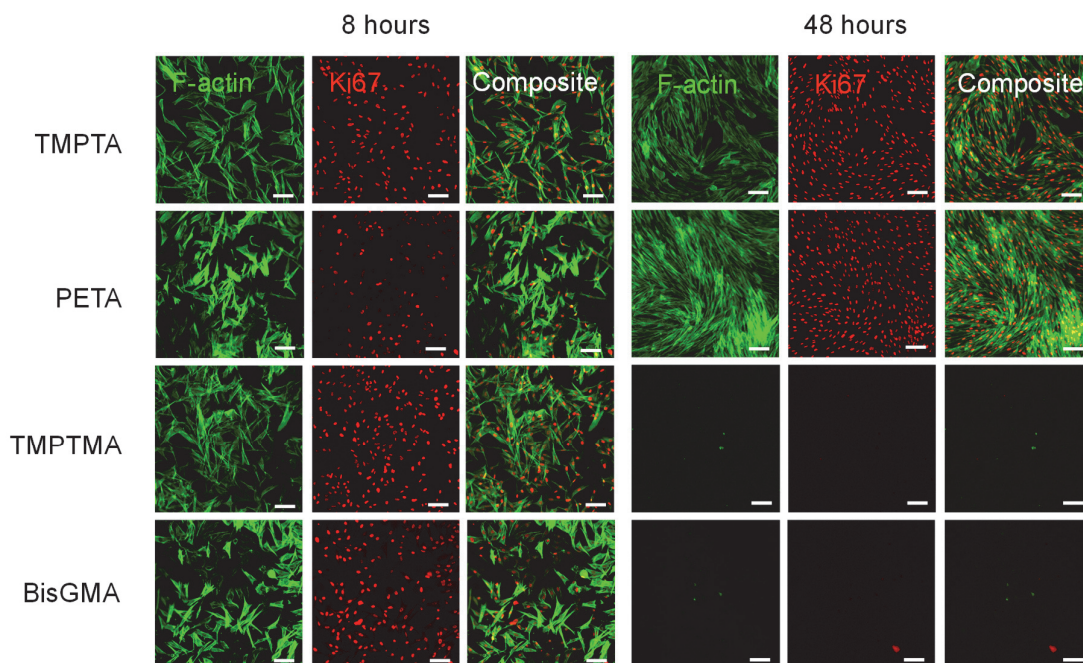


**Figure S3.** Confluent DPSCs under serum-free conditions express proliferation marker Ki67. Confocal microscopy of Ki67 immunostaining (red) and F-actin (green) at 8 and 48 hours on TMPTA, PETA, TMPTMA, and BisGMA, scale bar 100  $\mu\text{m}$ .

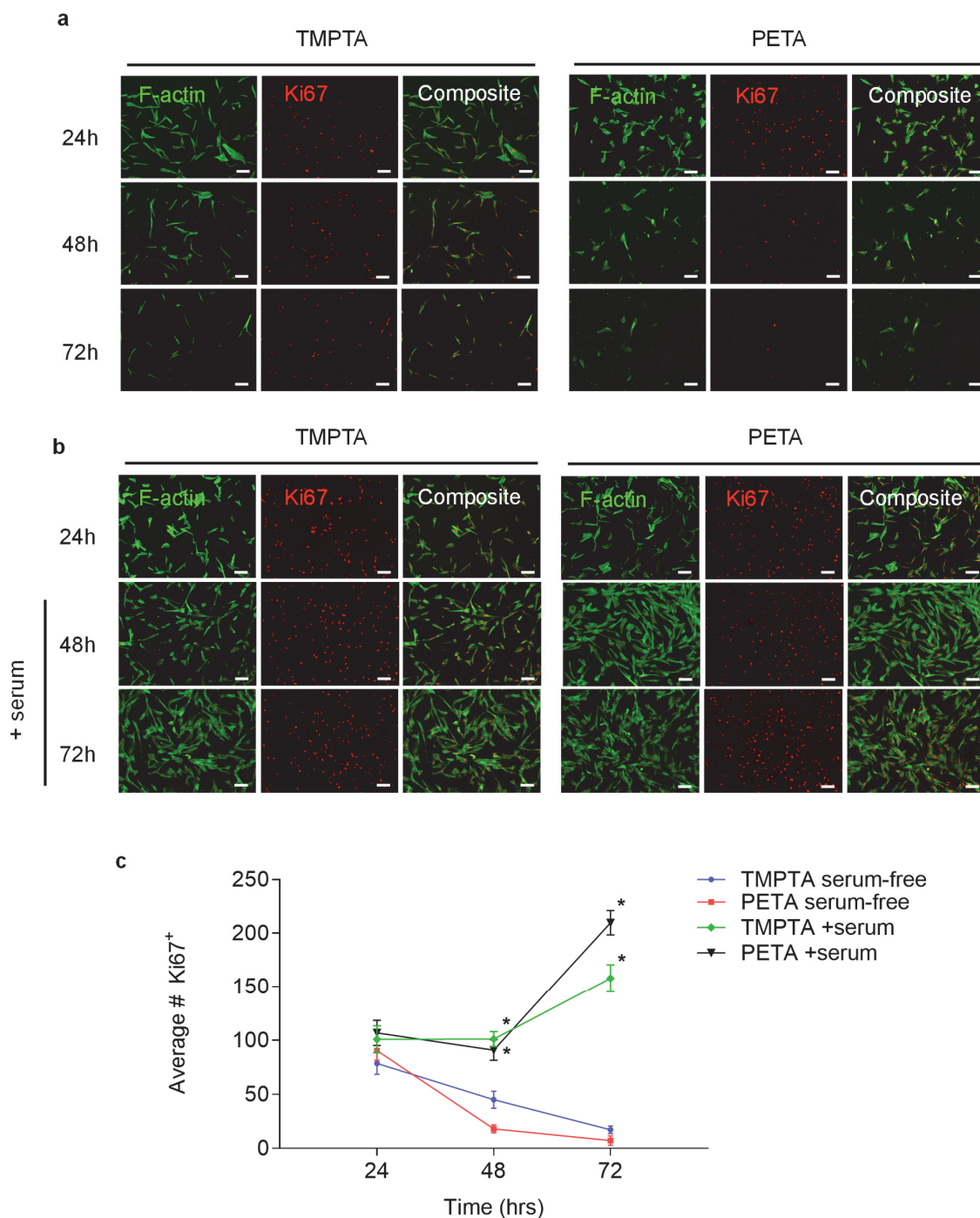


**Figure S4.** DPSCs maintain expression of proliferation marker Ki67 over 72 hours in serum-containing media. a) DPSCs seeded at subconfluent density ( $2.5 \times 10^4$  cells/cm<sup>2</sup>) on TMPTA and PETA in serum-free media show a reduction in Ki67 expression over 72 hours, as shown by fluorescence imaging of cells stained for F-actin (green) and Ki-67 (red). Scale bar 100  $\mu$ m. b) DPSCs on TMPTA and PETA in serum-containing media continued to proliferate over 72



hours. DPSCs were adhered at low seeding density ( $2.5 \times 10^4$  cells/cm<sup>2</sup>) initially in serum-free media, which was replaced at 24 hours with media containing 10% FBS. Fluorescence imaging of Ki67 (red) and F-actin (green) staining show the growth and recovery of Ki67+ cells. Scale bar 100  $\mu$ m. c) Quantification of average number of Ki67+ cells at 24, 48 and 72 hours on TMPTA and PETA, \* statistically significant difference from TMPTA-serum free condition,  $p < 0.05$ ,  $n \geq 8$ .

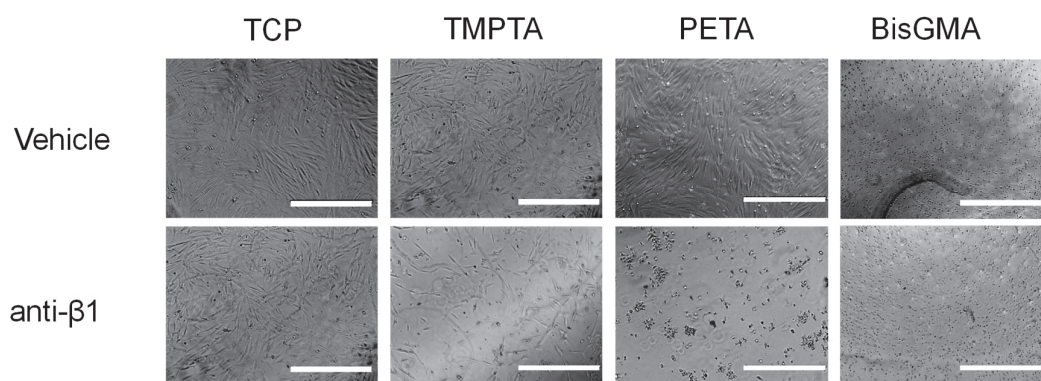


**Figure S5.** DPSCs adhere to and remain viable on triacrylates in an integrin-dependent manner. Phase images at 8 and 48 hours showed cells did not remain adhered on the triacrylates TMPTA and PETA, as well as BisGMA, when treated with an anti- $\beta$ 1 antibody to block the integrin  $\beta$ 1 receptor subunit, while it had no significant effect on the tissue culture control TCP. Scale bar 400  $\mu$ m.



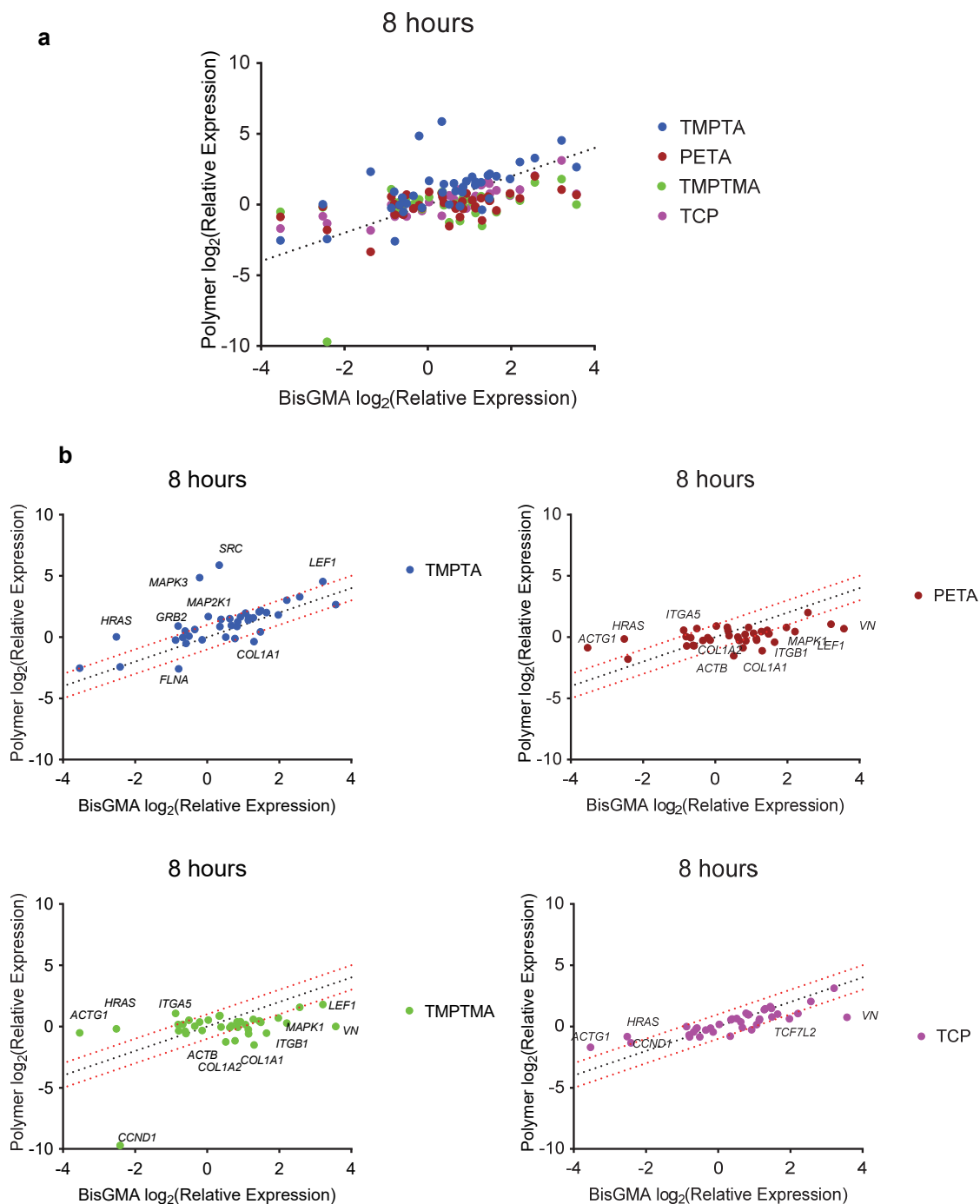


**Figure S6.** Gene expression analysis of DPSCs adhered after 8 hours to TCP, TMPTA, PETA, TMPTMA, TCP relative to BisGMA control. a) Differential expression of gene markers of  $\beta 1$  integrin signaling from a commercial gene array, using the BioRad PrimePCR Integrin Outside-In Signaling 384-well plate, normalized to GAPDH,  $n=2$ . Dotted line indicates unity

between polymer and BisGMA. b) Scatterplots used to identify differentially expressed genes (defined as above 2-fold threshold).

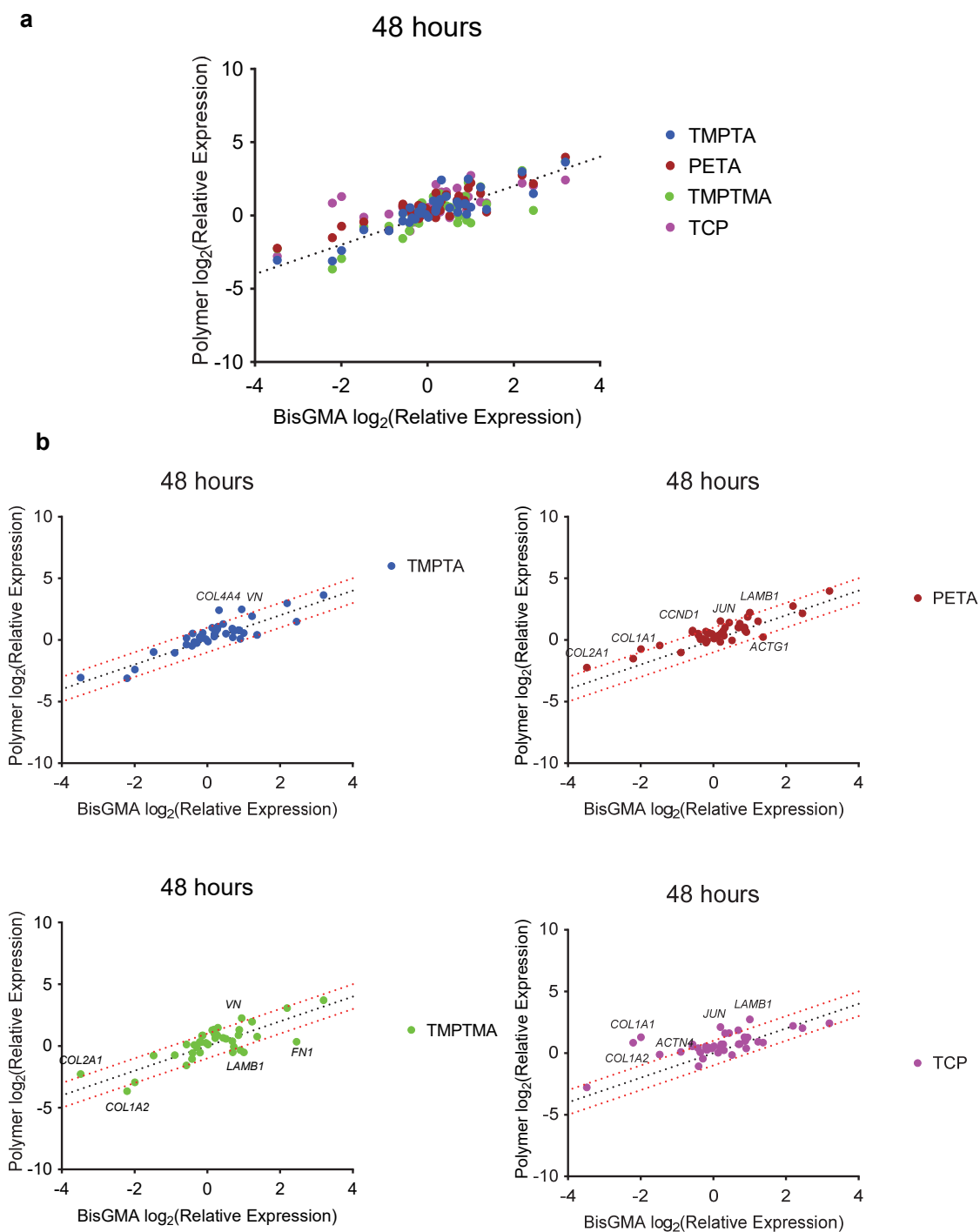


**Figure S7.** Gene expression analysis of DPSCs adhered after 48 hours to TCP, TMPTA, PETA, TMPTMA, and TCP relative to BisGMA control. a) Differential expression of gene

markers of  $\beta 1$  integrin signaling from a commercial gene array, using the BioRad PrimePCR Integrin Outside-In Signaling 384-well plate, normalized to GAPDH, n=2. Dotted line indicates unity between polymer and BisGMA. b) Scatterplots used to identify specific differentially expressed genes (defined as above 2-fold threshold).

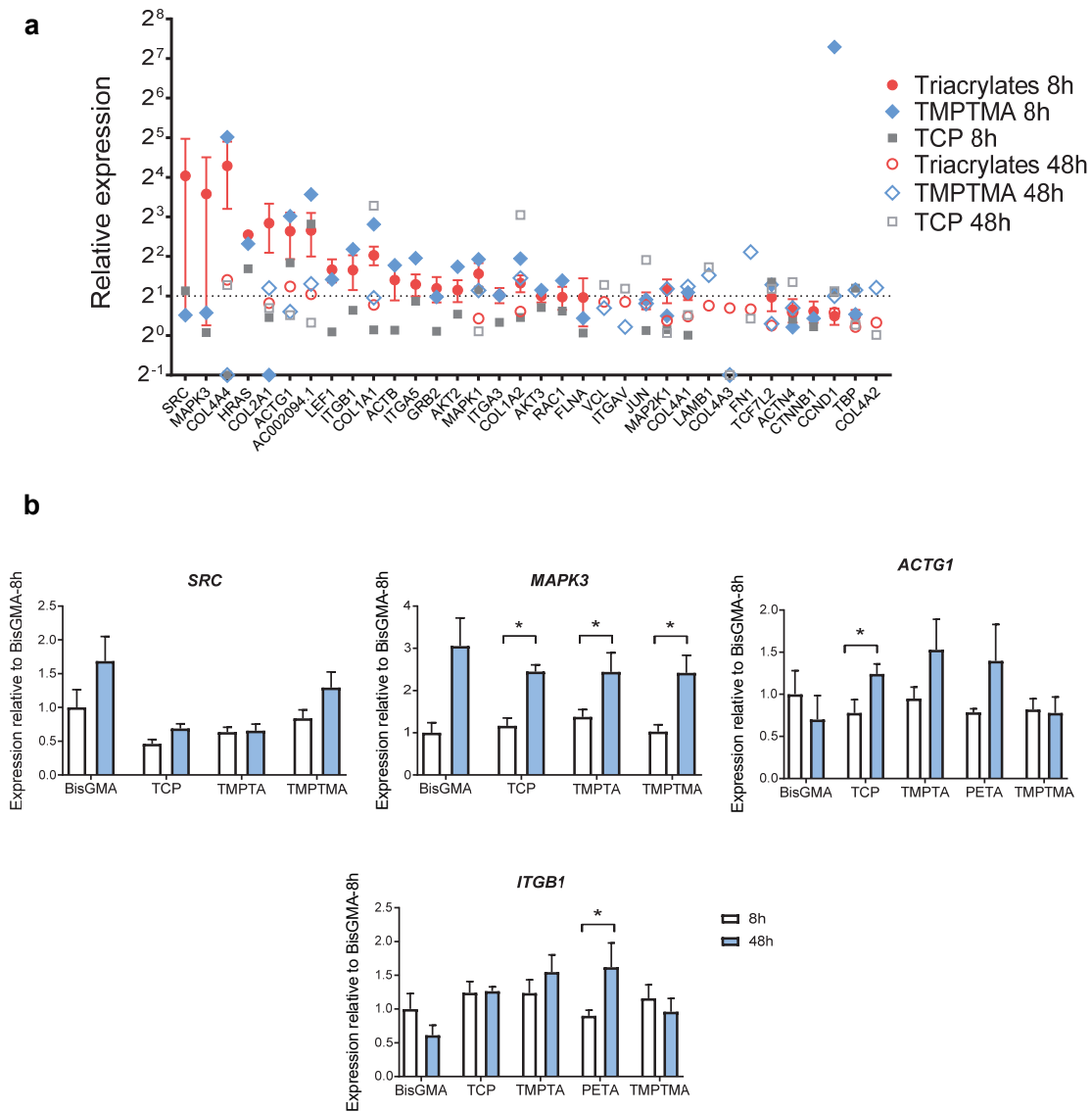


**Figure S8.** Candidate genes regulated by materials conditions. a) Ranked absolute relative gene expression of DPSCs adhered after 8 and 48 hours to TCP, triacrylates (mean of TMPTA and PETA), TMPTMA, and TCP, normalized to BisGMA control at 8 hours and GAPDH from the BioRad PrimePCR Integrin Outside-In Signaling gene array. b) Confirmation of

specific candidate genes by qPCR, in particular *SRC*, *MAPK3*, *ACTG1*, and *ITGB1* expression in DPSCs on BisGMA, TCP, TMPTA, PETA, and TMPTMA after 8 and 48 hours, normalized to BisGMA control at 8 hours and GAPDH, \* statistically significant difference, two-way ANOVA,  $p < 0.05$ ,  $n > 3$ .

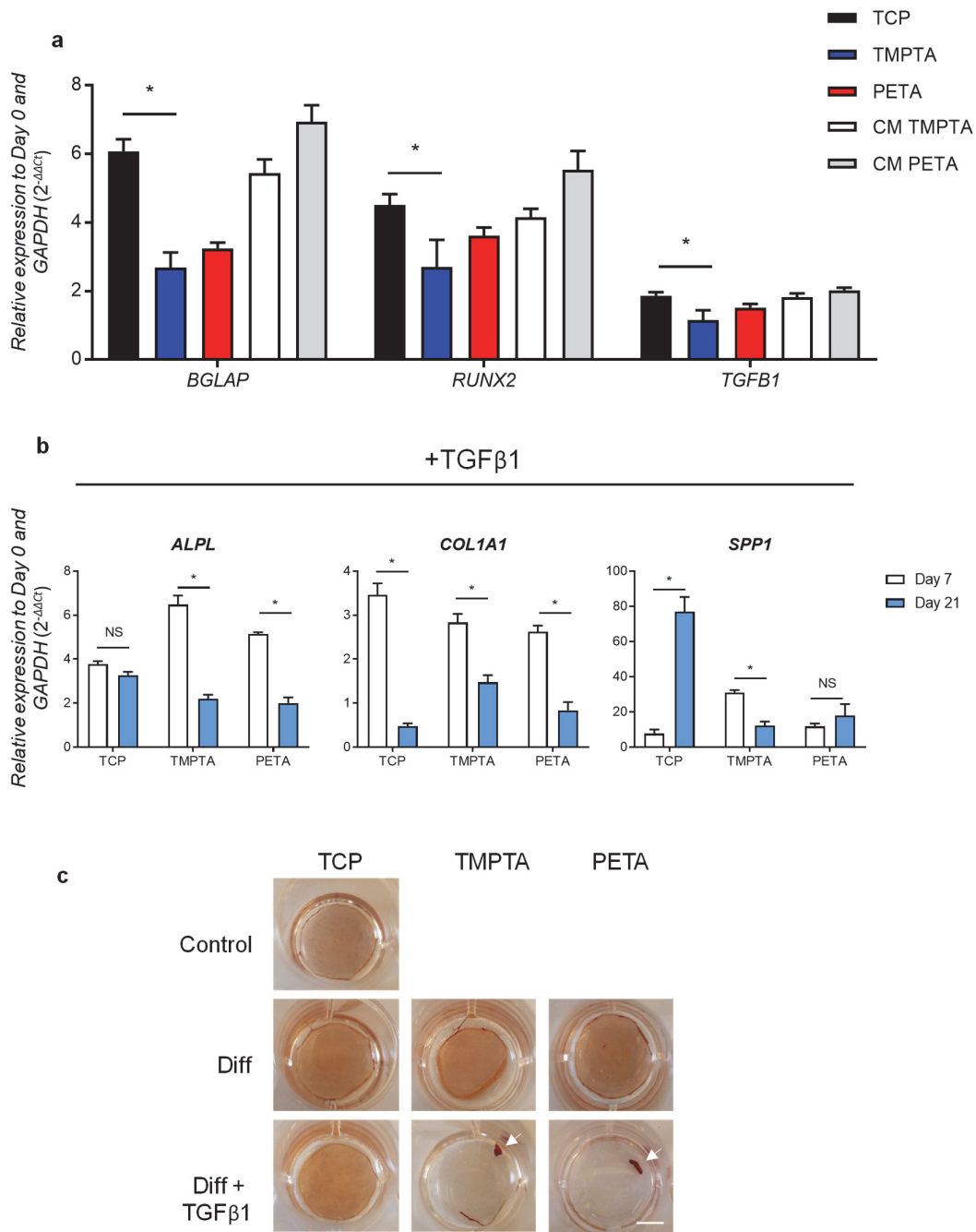


**Figure S9.** Gene expression of DPSCs on material conditions after long-term culture. a)

Relative gene expression of osteocalcin (*BGLAP*), *RUNX2*, and *TGFB1* in DPSCs on TCP,

TMPTA and PETA after 21 days in serum-free media, as well as cells on TCP exposed to conditioned media from TMPTA and PETA (CM), \* statistically significant difference, two-way ANOVA,  $p < 0.05$ ,  $n > 3$ . b) Relative expression of alkaline phosphatase (*ALPL*), collagen, type I (*COL1A1*), and osteopontin (*SPPI*) in DPSCs when cultured 7 and 21 days in osteogenic media with the addition of TGF $\beta$ 1 on TCP, TMPTA, and PETA, normalized by GAPDH and Day 0, \*statistically significant difference, two-way ANOVA,  $p > 0.05$ ,  $n = 3$ . c) Alizarin red staining of DPSCs on TCP, TMPTA, and PETA at 14 days under osteogenic conditions with (Diff + TGF $\beta$ 1) or without (Diff) growth factor TGF $\beta$ 1. DPSCs in TGF $\beta$ 1-media contract into a cluster of cells on TMPTA and PETA (white arrow). Scale bar 5 mm.

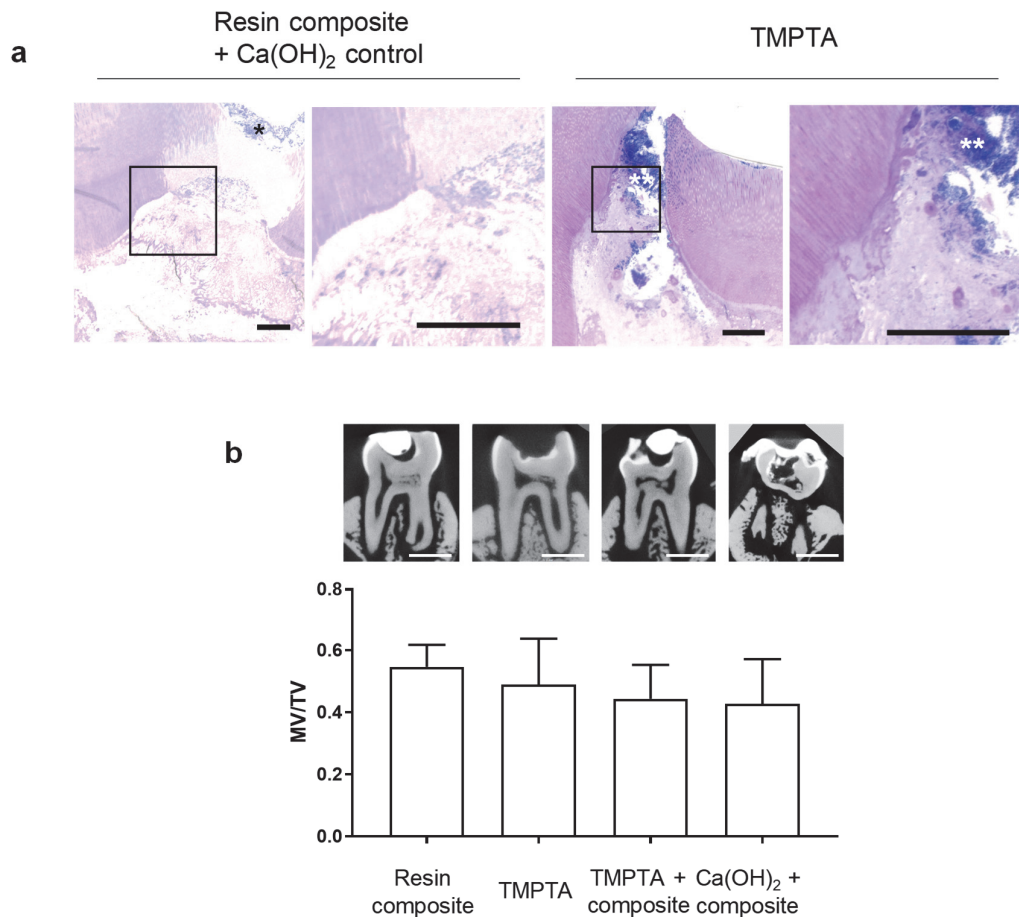


**Figure S10.** a) Hard tissue histological sections of TMPTA in direct contact with molar pulp defect at 8-weeks after injury (white asterisks), compared to control of calcium hydroxide paste and commercial dental resin composite (black asterisk). Scale bar 100  $\mu$ m. b) MicroCT

analysis of dental pulp calcifications. MicroCT images and mineralized-volume to total-volume ratio, as measured at 8 weeks for treatment with commercially available dental resin composite, composite + calcium hydroxide paste, TMPTA, or TMPTA + commercial resin composite. Scale bar 1 mm. No statistically significant differences between groups, one-way ANOVA,  $p > 0.05$ ,  $n = 2$ .

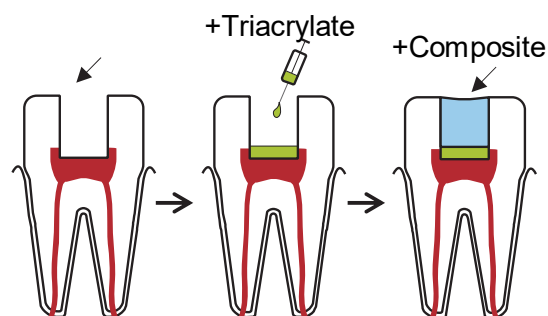


**Figure S11.** Proposed clinical application of triacrylate-based dental material to treat dental pulp injury following partial resection of pulp tissue (red) in molars and application of regenerative therapy (arrow). Triacrylate biomaterial (green) is placed in direct contact with treated pulp tissue to restore the dentin-pulp interface, because it supports DPSC regenerative behavior, and then is light-cured using traditional visible-light irradiation. Proper dental form and function are restored with a traditional dental composite material (blue). Alternatively, triacrylate-based materials could be used to develop one-step bio-instructive dental composite filling materials that are compatible with the dental pulp cells, as well as restore the tooth.



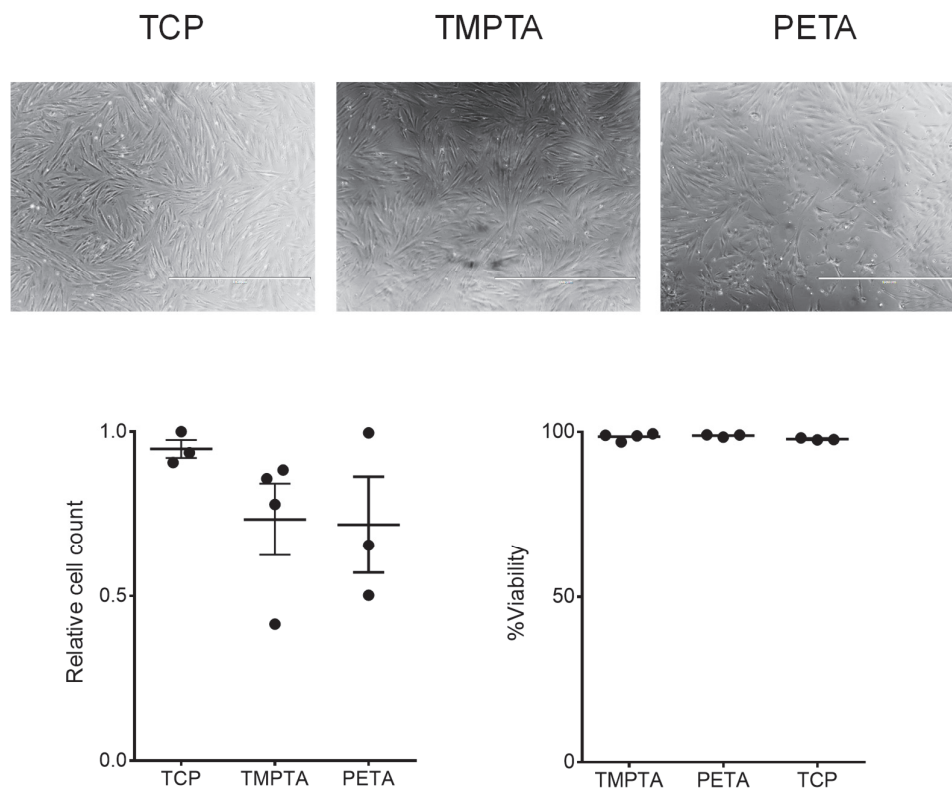


**Figure S12.** Triacrylate polymers TMPTA and PETA promoted adhesion of primary human periodontal ligament fibroblasts similar to tissue culture control (TCP). Phase images show confluent monolayers, scale bar 1 mm. Quantification of cell number, relative to highest cell number, and cell viability after 48 hours in serum-free media.

**Table S1.** Monomer list for polymer microarray

Monomer chemical name
Glycidyl methacrylate
N-(Butoxymethyl)acrylamide
N-Hydroxyethyl acrylamide
Benzyl 2-n-propyl acrylate
Norbornyl methacrylate
Isobornyl methacrylate
Methylthioethyl methacrylate
Caprolactone 2-(methacryloyloxy)ethyl ester
Hexadecafluoro-9-(trifluoromethyl)decyl acrylate
N-(Isobutoxymethyl)acrylamide

---

Tetrahydrofurfuryl acrylate  
Hexafluoropent-1,5-diyl diacrylate  
Tert-butylcyclohexylacrylate  
Tricyclodecane-dimethanol diacrylate  
Butanediol-1,3 diacrylate  
Poly(ethylene glycol) methyl ether acrylate  
N-[2-(1H-indol-3-yl)ethyl]acrylamide  
N-[Tris(hydroxymethyl)methyl]acrylamide  
N-(3-Methoxypropyl)acrylamide  
Ter-butyl methacrylate  
Stearyl methacrylate  
Phenyl methacrylate  
Isodecyl methacrylate  
Acryloyloxy- $\beta$ , $\beta$ -dimethyl- $\gamma$ -butyrolactone  
Poly(ethylene glycol) phenyl ether acrylate  
Hydroxypropyl acrylate  
Dimethylamino-propyl acrylate  
Isobutyl acrylate  
Hydroxypivalyl hydroxypivalate bis[6-(acryloyloxy)hexanoate]  
Tetra(ethylene glycol) diacrylate  
Di(ethylene glycol) diacrylate  
Acrylamide  
N-Phenylmethacrylamide  
Tri(ethylene glycol) methyl ether methacrylate  
Glycerol dimethacrylate  
Isobutyl methacrylate  
Lauryl methacrylate  
t-Butyl cyclohexyl methacrylate  
Caprolactone 2-(methacryloyloxy)ethyl ester  
Poly(propylene glycol) acrylate  
Glycerol propoxylate triacrylate  
Isodecyl acrylate  
Isooctyl acrylate  
Trimethylolpropane benzoate diacrylate  
3-Hydroxy-2,2-dimethylpropyl 3-hydroxy-2,2-dimethylpropionate diacrylate  
Ethylene glycol dimethacrylate  
1,4-Bis(acryloyl)piperazine  
N-(1,1,3,3-tetramethylbutyl)acrylamide  
Hydroxybutyl methacrylate  
Acryloyloxy-2-hydroxypropyl methacrylate  
Decyl methacrylate  
Ethylene glycol phenyl ether methacrylate  
Diethylaminoethyl methacrylate  
Ethylhexyl methacrylate

---

---

Pentaerythritol triacrylate  
N-Methylmethacrylamide  
Di(ethylene glycol) 2-ethylhexyl ether acrylate  
Lauryl acrylate  
Hexanediol ethoxylate diacrylate  
Bisphenol A ethoxylate diacrylate  
Dimethylamino-ethyl acrylate  
N-(4-Hydroxyphenyl)methacrylamide  
Methacrylamide  
N-[3-(Dimethylamino)propyl]acrylamide  
Vinyl methacrylate  
Cyclohexyl methacrylate  
Ethylene glycol methyl ether methacrylate  
Ethylhexyl methacrylate  
Tridecafluoro-2-hydroxynonyl acrylate  
Poly(propylene glycol) methyl ether acrylate  
Glycidyl acrylate  
Benzyl acrylate  
Epoxidized acrylate  
Ethylene glycol diacrylate  
Hexamethylene diacrylate  
Neopentyl glycol diacrylate  
N,N'-Ethylenebisacrylamide  
Sulfopropyl acrylate potassium salt  
Di(ethylene glycol) methyl ether methacrylate  
Butyl methacrylate  
Tetrahydrofurfuryl methacrylate  
Poly(ethylene glycol) methyl ether methacrylate  
Poly(ethylene glycol) methacrylate  
Hexyl methacrylate  
Hydroxy-3-phenoxypropyl acrylate  
Hydroxy-3-phenoxypropyl acrylate  
Di(ethylene glycol) ethyl ether acrylate  
Hexyl acrylate  
Glycerol 1,3-diglycerolate diacrylate  
Neopentyl glycol propoxylate diacrylate  
Ethylene glycol methyl ether acrylate  
Diacetone acrylamide  
N-(Hydroxymethyl)acrylamide  
Butoxyethyl methacrylate  
tetraethyleneglycol dimethacrylate  
Furfuryl methacrylate  
Tert-butylamino-ethyl methacrylate  
Ethylene glycol dicyclopentenyl ether methacrylate

---

Tri(ethylene glycol) dimethacrylate  
 Butylamino carbonyl oxy ethyl acrylate  
 Trimethylolpropane ethoxylate triacrylate  
 Poly(propylene glycol) 4-nonylphenyl ether acrylate  
 Trimethylhexyl acrylate  
 Poly(propylene glycol) diacrylate  
 Trimethylolpropane ethoxylate methyl ether diacrylate  
 [2-(Methacryloyloxy)ethyl]dimethyl-(3-sulfopropyl) ammonium hydroxide  
 N-tert-Butylacrylamide  
 mono-2-(Methacryloyloxy)ethyl succinate  
 N-[3-(Dimethylamino)propyl]methacrylamide  
 Methyl 3-hydroxy-2-methylenebutyrate  
 Methacryloyloxy)ethyl acetoacetate  
 Benzyl methacrylate  
 Ethyl-cis-B-cyano-acrylate  
 Hydroxybutyl acrylate  
 Trimethylolpropane propoxylate triacrylate  
 Isobornyl acrylate  
 Propargyl acrylate  
 Butanediol diacrylate  
 Methyl-1,2-ethanediyl bis[oxy(methyl-2,1-ethanediyl)]diacrylate

**Table S2.** BioRad PrimePCR Integrin Outside-In Signaling H384 Plate

Gene	Gene Name	PrimePCR ID
<i>ACTB</i>	actin, beta	qHsaCED0036269
<i>ACTG1</i>	actin, gamma 1	qHsaCED0005010
<i>ACTN1</i>	actinin, alpha 1	qHsaCED0002731
<i>ACTN4</i>	actinin, alpha 4	qHsaCID0012278
<i>CTNNB1</i>	catenin (cadherin-associated protein), beta 1, 88kDa	qHsaCID0010363
<i>COL1A1</i>	collagen, type I, alpha 1	qHsaCED0002181
<i>COL1A2</i>	collagen, type I, alpha 2	qHsaCED0003988
<i>COL2A1</i>	collagen, type II, alpha 1	qHsaCED0001057
<i>COL4A1</i>	collagen, type IV, alpha 1	qHsaCID0010223
<i>COL4A2</i>	collagen, type IV, alpha 2	qHsaCED0004426
<i>COL4A3</i>	collagen, type IV, alpha 3 (Goodpasture antigen)	qHsaCID0013308
<i>COL4A4</i>	collagen, type IV, alpha 4	qHsaCID0016411
<i>CCND1</i>	cyclin D1	qHsaCID0013833
<i>FNI</i>	fibronectin 1	qHsaCID0012349
<i>FLNA</i>	filamin A, alpha	qHsaCID0010844
<i>GAPDH</i>	glyceraldehyde-3-phosphate dehydrogenase	qHsaCED0038674
<i>GSK3B</i>	glycogen synthase kinase 3 beta	qHsaCID0010097
<i>GRB2</i>	growth factor receptor-bound protein 2	qHsaCED0004795
<i>HPRT1</i>	hypoxanthine phosphoribosyltransferase 1	qHsaCID0016375
<i>ITGA2</i>	integrin, alpha 2	qHsaCID0016134
<i>ITGA3</i>	integrin, alpha 3	qHsaCID0010823
<i>ITGA5</i>	integrin, alpha 5	qHsaCID0021495
<i>ITGAV</i>	integrin, alpha V	qHsaCID0006233
<i>ITGB1</i>	integrin, beta 1	qHsaCED0005248
<i>ILK</i>	integrin-linked kinase	qHsaCED0038739
<i>JUN</i>	jun proto-oncogene	qHsaCED0018770
<i>LAMB1</i>	laminin, beta 1	qHsaCID0006489

<i>LEF1</i>	lymphoid enhancer-binding factor 1	qHsaCED0001977
<i>MAPK1</i>	mitogen-activated protein kinase 1	qHsaCID0006818
<i>MAPK3</i>	mitogen-activated protein kinase 3	qHsaCID0010939
<i>MAP2K1</i>	mitogen-activated protein kinase kinase 1	qHsaCID0011553
<i>gDNA</i>	PrimePCR DNA Contamination Control Assay	qHsaCtID0001004
<i>PCR</i>	PrimePCR Positive Control Assay	qHsaCtID0001003
<i>RT</i>	PrimePCR Reverse Transcription Control Assay	qHsaCtID0001001
<i>RQ1</i>	PrimePCR RNA Quality Assay	qHsaCtID0001002
<i>RQ2</i>	PrimePCR RNA Quality Assay	qHsaCtID0001002
<i>PTK2</i>	PTK2 protein tyrosine kinase 2	qHsaCED0001879
<i>RAC1</i>	ras-related C3 botulinum toxin substrate 1 (rho family, small GTP binding protein Rac1)	qHsaCED0001330
<i>TBP</i>	TATA box binding protein	qHsaCID0007122
<i>TCF7L2</i>	transcription factor 7-like 2 (T-cell specific, HMG-box)	qHsaCID0012510
<i>AKT1</i>	v-akt murine thymoma viral oncogene homolog 1	qHsaCID0011338
<i>AKT2</i>	v-akt murine thymoma viral oncogene homolog 2	qHsaCED0037964
<i>AKT3</i>	v-akt murine thymoma viral oncogene homolog 3	qHsaCID0036448
<i>HRAS</i>	v-Ha-ras Harvey rat sarcoma viral oncogene homolog	qHsaCED0023908
<i>VCL</i>	vinculin	qHsaCID0020885
<i>AC002094.1</i>	Vitronectin	qHsaCED0001902
<i>RAF1</i>	v-raf-1 murine leukemia viral oncogene homolog 1	qHsaCED0001147
<i>SRC</i>	v-src sarcoma viral oncogene homolog (avian)	qHsaCED0004489

**Table S3.** BioRad PrimePCR assays for qPCR

Gene	Gene Name	PrimePCR ID
<i>AC002094.1 (VN)</i>	Vitronectin	qHsaCED0001902
<i>ACTA2</i>	Smooth muscle actin	qHsaCID0013300
<i>ACTG1</i>	Actin, gamma 1	qHsaCED0005010
<i>ALPL</i>	Alkaline phosphatase	qHsaCED0045991
<i>BGLAP</i>	Osteocalcin	qHsaCED0038437
<i>CCND1</i>	Cyclin D1	qHsaCID0013833
<i>COL1A1</i>	Collagen, type I, alpha 1	qHsaCED0043248
<i>COL2A1</i>	Collagen, type II, alpha 1	qHsaCED0001057
<i>COL4A4</i>	Collagen, type IV, alpha 4	qHsaCID0016411
<i>DSPP</i>	Dentin sialophosphoprotein	qHsaCED0002962
<i>GAPDH</i>	Glyceraldehyde-3-phosphate dehydrogenase	qHsaCED0038674
<i>HRAS</i>	Harvey rat sarcoma viral oncogene homolog	qHsaCED0023908
<i>ITGB1</i>	integrin, beta 1	qHsaCED0005248
<i>LEF1</i>	Lymphoid enhancer-binding factor 1	qHsaCED0001977
<i>MAPK3</i>	Mitogen-activated protein kinase 3	qHsaCID0010939
<i>RUNX2</i>	Runx-2	qHsaCED0044067
<i>SPP1</i>	Secreted phosphoprotein 1, osteopontin	qHsaCED0057074
<i>STC1</i>	Stanniocalcin	qHsaCID0006115
<i>SRC</i>	v-src sarcoma viral oncogene homolog (avian)	qHsaCED0004489